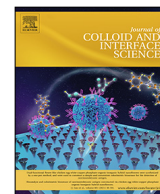




Contents lists available at ScienceDirect

Journal of Colloid and Interface Science

journal homepage: www.elsevier.com/locate/jcis

Switchable β -lactoglobulin (BLG) adsorption on protein resistant oligo (ethylene glycol) (OEG) self-assembled monolayers (SAMs)



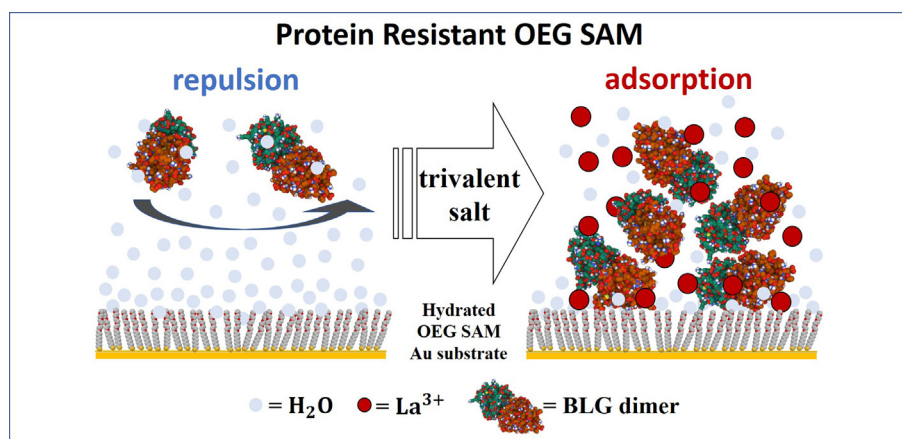
Maximilian W.A. Skoda^{a,1}, Nina F. Conzelmann^{b,1}, Madeleine R. Fries^b, Lara F. Reichart^b, Robert M.J. Jacobs^c, Fajun Zhang^b, Frank Schreiber^{b,*}

^a STFC, ISIS Neutron and Muon Source, Rutherford Appleton Laboratory, Harwell Campus, Didcot OX11 0QX, UK

^b Institut für Angewandte Physik, Universität Tübingen, Auf der Morgenstelle 10, Tübingen 72076, Germany

^c Department of Chemistry, Chemistry Research Laboratory, University of Oxford, South Parks Road, Oxford OX1 3TA, UK

GRAPHICAL ABSTRACT



ARTICLE INFO

Article history:

Received 14 May 2021

Revised 7 July 2021

Accepted 3 August 2021

Available online 8 August 2021

Keywords:

Protein adsorption

OEG SAMs

Protein resistance

ABSTRACT

Hypothesis: Although protein adsorption at an interface is very common and important in biology and biotechnology, it is still not fully understood – mainly due to the intricate balance of forces that ultimately control it. In food processing (and medicine), controlling and manipulating protein adsorption, as well as avoiding protein adsorption (biofilm formation or membrane fouling) by the production of protein-resistant surfaces is of substantial interest. A major factor conferring resistance towards protein adsorption to a surface is the presence of tightly bound water molecules, as is the case in oligo ethylene glycol (OEG)-terminated self-assembled monolayers (SAMs). Due to strong attractive protein-protein and protein-surface interactions observed in systems containing trivalent salt ions, we hypothesize that these conditions may lead to a breakdown of protein resistance in OEG SAMs.

Abbreviations: QCM-D, quartz crystal microbalance with dissipation; BLG, β -lactoglobulin; c^* , boundary between regime I and II; c^{**} , boundary between regime II and III; Ca²⁺, calcium(2+) ion; CI, confidence interval; c_p , protein concentration; c_s , salt concentration; $d_{\text{QCM-D}}$, adsorbed protein layer thickness determined by QCM-D; Δf , QCM-D frequency shift; F , measured QCM-D frequency; ΔD , QCM-D dissipation shift; D , measured QCM-D dissipation; D₂O(l), heavy water; d_{NR} , adsorbed protein layer thickness determined by neutron reflectivity; H₂O(l), normal water; Hydr., hydration of adsorbed layer; λ , wavelength; La³⁺, lanthanum(3+) ion; LaCl₃, lanthanum chloride; LLPS, liquid-liquid phase separation; NR, neutron reflectivity; Q , momentum transfer; RC, re-entrant condensation; SiO₂, silicon dioxide; SLD, scattering length density; σ , layer roughness; θ , incident angle.

* Corresponding author.

E-mail address: frank.schreiber@uni-tuebingen.de (F. Schreiber).

¹ These authors contributed equally to the paper.

<https://doi.org/10.1016/j.jcis.2021.08.018>

0021-9797/© 2021 Published by Elsevier Inc.

Trivalent ions
QCM-D
Neutron reflectometry

Experiments: We studied the adsorption behavior of BLG in the presence of a lanthanum(III) chloride (LaCl_3) at concentrations of 0, 0.1, 0.8 and 5.0 mM on normally protein resistant triethylene glycol-terminated (EG₃) SAMs on a gold surface. We used quartz-crystal microbalance with dissipation (QCM-D) and neutron reflectivity (NR) to characterize the morphology of the interfacial region of the SAM.

Findings: We demonstrate that the protein resistance of the EG₃ SAM breaks down beyond a threshold salt concentration c^* and mirrors the bulk behaviour of this system, showing reduced adsorption beyond a second critical salt concentration c^{**} . These results demonstrate for the first time the controlled switching of the protein-resistant properties of this type of SAM by the addition of trivalent salt.

© 2021 Published by Elsevier Inc.

1. Introduction

The prevention or control of protein adsorption plays an important role in many areas of our daily life ranging from biotechnology through medicine and pharmaceutical science to biophysics. Protein adsorption at interfaces is considered to be one of the first steps in coagulation processes in blood [1] or in transmembrane signaling. Protein adsorption can also promote inflammation cascades, bacteria and cell adhesion or membrane fouling processes [2]. Particularly in food processing, membrane fouling is a major obstacle in purification and filtration of many products including milk and whey [3,4]. Upon fouling, the flux declines resulting in prolonged process times and a decreased purification efficiency [5], which leads to increased energy and cleaning costs. Factors such as protein concentration, pH, heat treatment and the addition of salts have been identified as key factors for the surface activity of proteins [6], while surface properties such as hydrophilicity, charge and roughness influence fouling resistance [7].

One attempt to circumvent such unwanted behavior is the use of poly(ethylene glycol) (PEG)- or oligo(ethylene glycol) (OEG)-terminated self-assembled monolayer (SAM)-grafting to create surfaces resistant to protein adsorption; these are extensively described in the literature [8–16]. It is considered that repulsive steric forces created by the SAM and coupled/structured interfacial water molecules produce the protein-repellent properties [10,17–19]. If a macromolecule approaches the surface, the conformational degrees of freedom of the PEG molecules are dramatically reduced, which causes these repulsive forces between the PEG molecules and the proteins [20]. SAM molecules with only short ethylene glycol (EG) ($-\text{CH}_2-\text{CH}_2-\text{O}-$) units in a laterally densely packed layer have a reduced steric repulsion force due to conformational constraints. This indicates that the chain length and number of EG groups is another critical factor. Harder et al. [12] furthermore proposed that the ability of water to integrate into the SAM is another key aspect. Here, the internal hydrophilicity (i.e. water integrating into the SAM) as well as the hydrophilicity of the SAM termination (i.e. water molecules can approach and access the SAM) seem to be critical properties. The penetration of water molecules in the layer is directly linked to the packing density of the SAM. A higher content of water in the layer indicates a more relaxed packing of SAM molecules and a higher chance to achieve protein resistance [21]. The initially well-ordered SAMs (all-trans structure) become disordered in water (helical structure) due to the strong interactions of water with the polar ether groups allowing water to penetrate the layer more easily [22,23].

Furthermore, several studies revealed that SAMs containing OEG/PEG exhibit a negative electrostatic potential when immersed in water [9,24–26]. These charges are probably caused by hydroxide (OH^-) ions in solution adsorbing to the surface and inducing an electrostatic repulsive force. These studies revealed that it is not decisive whether the endgroup has a methoxy or hydroxy moiety,

therefore excluding deprotonation of the hydroxyl termination as the main source for possible negative charges of the layer [25]. Despite the likely presence of some charges associated with the SAM, a breakdown of protein resistance was not observed even in the presence of 1 M monovalent salt (NaCl) solution [27]. To date, no complete mechanism behind the prevention of protein adsorption in OEG based monolayers has yet been identified [18,28–32].

By contrast, in highly charged polymeric systems, such as grafted polyelectrolyte brushes and DNA, protein adsorption or repulsion can be modulated by variations in ionic strength [33,34].

In this study, we focus on the protein adsorption process on SAM-coated surfaces modulated by trivalent salts. We used SH $(\text{CH}_2)_{11}\text{EG}_3\text{OH}$ (EG_3OH) as a protein resistant SAM and BLG due to its model character (globular protein and net negatively charged), its high percentage in whey, and therefore its impact in food processing [35–37]. BLG is one of the most abundant proteins in whey and plays an important role not only in food processing, but also in pharmacology in drug production/creation [38]. We observe that the addition of a trivalent salt, here LaCl_3 , strongly influences the protein adsorption behavior on the EG_3OH functionalized surfaces. We used La^{3+} because of its important properties in manipulating protein adsorption [39,40] and its role as a pH-neutral model ion of other multivalent pH-dependent/sensitive ions naturally occurring in the human body (e.g. Al^{3+} , Fe^{3+}) [41,42]. Furthermore, our group has demonstrated that trivalent ions can be used to manipulate the protein phase behavior in the bulk and that protein-ion bridging can trigger cluster formation, re-entrant condensation and liquid-liquid phase separation (LLPS) [43]. Using the protein-salt system in the presence of a bare silicon dioxide surface, we have already observed re-entrant interface adsorption, which reflects the protein phase behavior in the bulk in an intriguing way [44].

Here, we demonstrate that the EG_3OH -functionalized surfaces lose their protein resistance towards BLG by the addition of a specific amount of trivalent salt (LaCl_3). The process of protein adsorption at the solid-liquid interface is monitored with a quartz-crystal microbalance with dissipation (QCM-D), and the detailed layer structure (i.e. density profile) is determined by neutron reflectivity (NR).

2. Results and discussion

In the following sections, using a protein resistant EG_3OH SAM, we present findings about the protein adsorption process and the layer morphology as a function of trivalent salt concentration (regimes I-III), as well as control measurements to validate our results. The findings will be interpreted and discussed (including error assessment) in Section 2.7. All thiol coated substrates used in the QCM-D measurements were characterized via contact angle, AFM and PMIRRAS measurements and a protein resistance test was

performed to determine the quality of the SAM layer. Only samples which had the right quality and properties associated with a protein-resistant SAM layer, were used for the subsequent adsorption measurements. An overview of the fitted adsorbed protein layer thickness and other parameters can be found in Table 1.

2.1. OEG SAMs characterization

While OEG SAMs are relatively easy to prepare, small changes in the deposition protocol can lead to changes (such as coverage variation, hydration level, defects etc) which in turn can affect the non-fouling properties. Furthermore, since we have used different substrates for NR and QCM-D measurements, we have thoroughly characterized all surfaces before and after OEG SAM formation. Details can be found in the supporting material. In particular, the surface morphology (roughness, defects etc) before and after OEG SAM formation was characterised by AFM (Figure S3), while the functionality of the SAM was assessed by contact angle measurements (Figure S2) and PM-IRRAS, using the characteristic C-O-C stretching mode, which is sensitive to SAM order and hydration (cf. Figure S4). Lastly, the protein resistance of each SAM used for QCM-D measurements was assessed by exposing the fresh SAM to a 5 mg/mL BLG solution without added salt (Figure S5).

2.2. Influence of trivalent salt on proteins in solution

Before addressing the adsorption behavior, it is useful briefly to summarize the bulk phase behaviour of the proteins as a function of the concentration c_s of trivalent ions. In bulk solution, three different **regimes (I-III)** delimited by two specific concentrations c^* and c^{**} are observed (Figure S1). For a BLG concentration of 5 mg/mL as used in this study, the critical salt concentrations, which separate the regimes are $c^* = 0.35$ mM and $c^{**} = 1.9$ mM. Below c^* , a transparent protein-salt solution with no visible protein clustering is observed, in which repulsive forces dominate the net negatively charged proteins (**regime I**). Increasing c_s above the first critical concentration c^* , leads to a weakening of the repulsive interactions, resulting in a turbid solution (**regime II**): the increased concentration of trivalent ions inverts the dominating electrostatic forces from repulsive to attractive due to increasing protein-ion bridging resulting in protein aggregation. Further increasing c_s leads to a phase transition from the turbid solution back to a transparent solution (**regime III**). Due to the increased binding of trivalent cations, the proteins undergo charge inversion, which results in weaker protein-protein interactions and re-entrant condensation (RC) (for details, see Figure S1 and Refs. [43,45]). This system also shows metastable LLPS as a time-dependent process in regime II after 1-2 h (for details, see [40]).

2.3. Effect of trivalent salt on OEG SAMs

OEG SAMs have been extensively characterised, as described in the introduction. While the presence of a highly hydrated region is a prerequisite for protein resistance of a surface [15,18,19,27,28,32], electrostatic interactions have also been proposed [24,26] as a contributing factor. The impact of monovalent salt via charge screening on the protein resistance of OEG SAMs has been investigated by our group [27] and others [14,25,46]. For the system presented in this work, in order to exclude a breakdown of protein resistance just by virtue of *monovalent* salt, we performed measurements with NaCl at similar ionic strength in order to assess the effect of monovalent salt on the current system. Control measurements confirmed sustained protein resistance in the presence of a NaCl solution of an ionic strength equal to that of LaCl₃ in regime II (see SI). The breakdown of protein resistance occurred only when trivalent salt was used.

Furthermore, the conformation and packing density of SAM molecules is crucial for sustained protein resistance [10,23]. More recently, trivalent salt solutions have been found to affect the properties of similar surfaces: Yu et al. [47,48] found that layers of polyelectrolyte brushes are highly affected by multivalent ions, leading to a brush collapse.

In order to assess possible changes of the EG₃OH SAM triggered by the addition of trivalent salt, we conducted salt only measurements before performing salt/protein mixtures measurements. We detected only minor changes in dissipation upon addition of different concentrations of salt (LaCl₃) without protein (Fig. 1), which indicates that the viscoelastic properties do not significantly change and it is likely that the hydration of the EG₃OH SAM is almost invariant. In the sample representing regime I, only a small change in Δf is observed, which could solely be explained by solution exchange (from pure water to salt solution) and the power-on of the pump. For the samples representing c_s in regimes II and III, a stronger change in Δf is observed: some of the La³⁺ ions possibly bind electrostatically to the terminal SAM EG groups, causing a slight mass increase. Even for these samples, ΔD is still rather low, indicating that LaCl₃ does not provoke substantial changes in the SAM. Hence, we can assume that the overall structure of the SAM is not significantly altered after the addition of the trivalent salt. However, it is not clear how many trivalent ions really adsorb to the layer since the molecular weight and the viscoelastic properties of La³⁺ ions are closely related to the properties of water as detected/measured by QCM-D [49]. If ion bridging is occurring, it is not yet established to which areas of the SAM molecules the La³⁺ ions bind. Most likely, due to its relatively small ionic radius of 0.116 nm [50], binding/association could occur on the EG groups (i.e. interior of the thiol layer), as well as the end group of the SAM (i.e. thiol/water interface).

2.4. Regime I: protein resistance (repulsive protein-protein interactions)

The QCM-D raw data (Fig. 2) show the smallest shifts in frequency (and dissipation) for those samples, in which no salt or a low concentration of salt ($c_s = 0.1$ mM in regime I) was used in a mixture with 5 mg/mL BLG in D₂O(l). Such small changes in Δf and ΔD in the range of 1 Hz or 1×10^{-6} , respectively, are on the level of the noise or background signal [51]. Furthermore, the change of the solvent from D₂O(l) to the protein-salt-D₂O(l) solution can cause small changes in frequency and dissipation due to the viscosity differences of the media [35,43].

In the context of this study, QCM-D and NR measurements showing only these minor changes during protein adsorption demonstrate that these surfaces should be considered essentially protein-repellent. This applies to measurements without salt and at low c_s of 0.1 mM. A protein layer thickness of $d_{\text{QCM-D}}(0 \text{ mM}) < 10$ Å and $d_{\text{QCM-D}}(0.1 \text{ mM}) < 10$ Å can be inferred, due to the fact that a QCM-D model including a protein layer did not fit the data satisfactorily. The NR fits for $c_s = 0.1$ mM (Fig. 3) revealed a 'dry' protein layer thickness, excluding the water coupled to the protein layer, of $d_{\text{NR}}(0.1 \text{ mM}) = 17$ Å, 95% CI [10,21] Å and a hydration of 99%, 95% CI [74%, 100%]. The small layer thickness at low c_s together with the high percentage of hydration (low volume fraction of protein) confirms the assumption that no significant amount of protein adsorbs on the SAM-coated surface. Additionally, after rinsing the QCM-D flow cell with water (after 1 h of adsorption), frequency and dissipation return to the initial value, indicating no irreversible protein adsorption. Additional information about layer properties can be extracted from dissipation shifts measured by QCM-D, in which a big shift indicates a highly viscoelastic layer compared to a small shift for a rigid and stiff layer

Table 1

Summary of layer morphology. Modeled thickness (d), roughness (σ_{NR}) and hydration of the protein layer on the surface coated with OEG based SAMs at different concentrations of LaCl_3 . Due to limited beamtime availability, no "No salt" NR data were taken. Errors for the QCM-D measurements represent standard deviation of at least three different samples, while the errors for the NR values represent the 95% confidence intervals of the posterior distributions based on MCMC sampling (as described in the Methods section).

OEG SAM: BLG layer thickness with LaCl_3 ($\pm 95\%$ CI for NR)					
Salt concentration c_s	$d_{\text{QCM-D}}$ (Å)		d_{NR} (Å)	σ_{NR} (Å)	Hydr. (%)
	$\text{H}_2\text{O(l)}$	$\text{D}_2\text{O(l)}$			
No salt	$<10^{\dagger}$	10 ± 7	–	–	–
NaCl control	$<10^{\dagger}$	$<10^{\dagger}$	$6_{0,0}^{10}$	7_3^{10}	86_{62}^{100}
0.1 mM (regime I)	$<10^{\dagger}$	10 ± 5	17_{10}^{21}	6_3^7	99_{74}^{100}
0.8 mM (regime II)	767 ± 196	697 ± 137	235_{198}^{332}	65_{51}^{91}	78_{69}^{91}
5.0 mM (regime III)	21 ± 16	63 ± 11	23_{10}^{38}	6_3^9	99_{86}^{100}

[†] QCM-D fits under these conditions did not yield meaningful results due to the very low frequency shift, such that no error bars could be extracted. This indicates that a model assuming a distinct layer is not appropriate and thus this suggests the absence of adsorption.

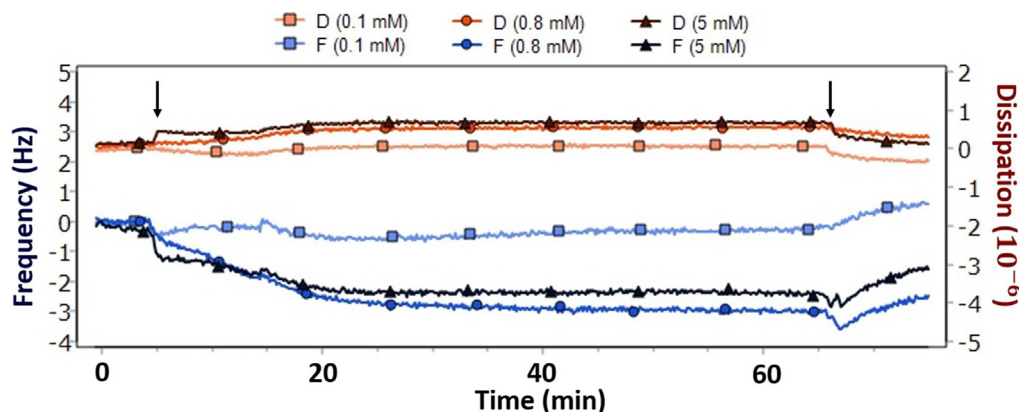


Fig. 1. QCM-D raw data on a EG_3OH coated gold surface with the frequency shifts (blue) and the dissipation shifts (red) of the 9th overtone. Different concentrations (c_s) of LaCl_3 with no protein in $\text{D}_2\text{O(l)}$ were used, reflecting the individual regimes in the complex phase diagram (0.1 mM $\hat{=}$ regime I, 0.8 mM $\hat{=}$ regime II and 5 mM $\hat{=}$ regime III, cf. Figure S1). The arrows indicate the injection of salt solution (~ 5 min) and pure solvent rinse (~ 65 min). Changes in frequency and dissipation are visible, but small, suggesting that the trivalent ions alone cannot account for the changes seen in the presence of proteins in regime II (see following sections).

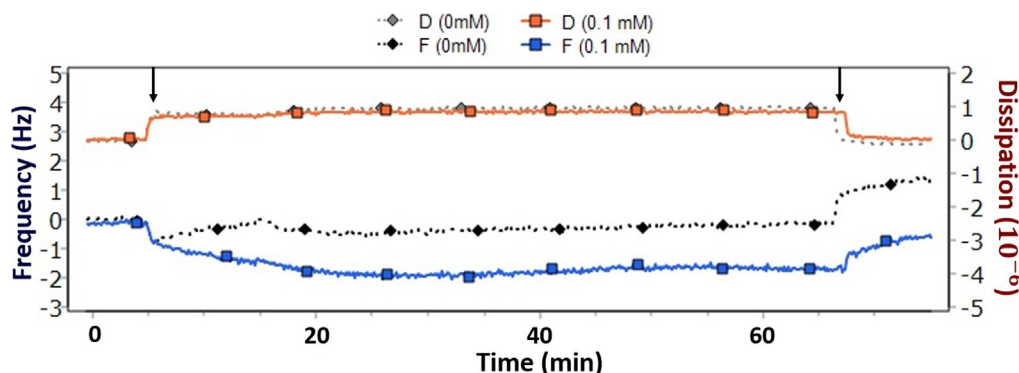


Fig. 2. QCM-D data without salt and regime I: The frequency shift (dotted black) and dissipation (dotted gray) for a 5 mg/mL BLG solution in $\text{D}_2\text{O(l)}$ without added salt. The frequency shift (blue) and the dissipation shifts (orange) of the 9th overtone show the system with 5 mg/mL of BLG in $\text{D}_2\text{O(l)}$ in the presence of 0.1 mM LaCl_3 . Arrows denote the injection of salt solution and pure solvent rinse, respectively. Both measurements show only minor frequency and dissipation shifts presumably caused by the medium change and background noise. This leads to the conclusion that the OEG SAM coated gold substrate resists protein adsorption at no salt and low salt concentration.

[35]. Here, the measured values of ΔD for the no salt and 0.1 mM measurements are in the range of $<1 \times 10^{-6}$ and therefore assumed to be caused only by the sub-phase change which is again supported by Δf and ΔD returning to the initial value after rinsing with pure water.

2.5. Regime II: Strong protein adsorption (attractive protein-protein interactions)

The strongest changes in the QCM-D data in (Δf and ΔD) were observed in regime II, at a salt concentration of 0.8 mM LaCl_3 .

Fig. 4 shows a sharp decrease in frequency to -250 Hz (accompanied by an equally steep rise in the dissipation) indicating a large amount of protein being adsorbed to the surface. This frequency drop corresponds to a modeled protein layer thickness of $d_{\text{QCM-D}}(0.8 \text{ mM}) = 767 \pm 196$ Å. The NR fitting (Fig. 5) confirmed the presence of a thick protein layer with a thickness of $d_{NR}(0.8 \text{ mM}) = 235$ Å, 95% CI [198, 332] Å and a hydration 78%, 95% CI [69%, 91%]. The protein layer roughness in regime II was 65 Å, 95% CI [51, 91] Å, which indicates a rough and diffuse protein interface. Such a layer could be formed by the adsorption of clusters or

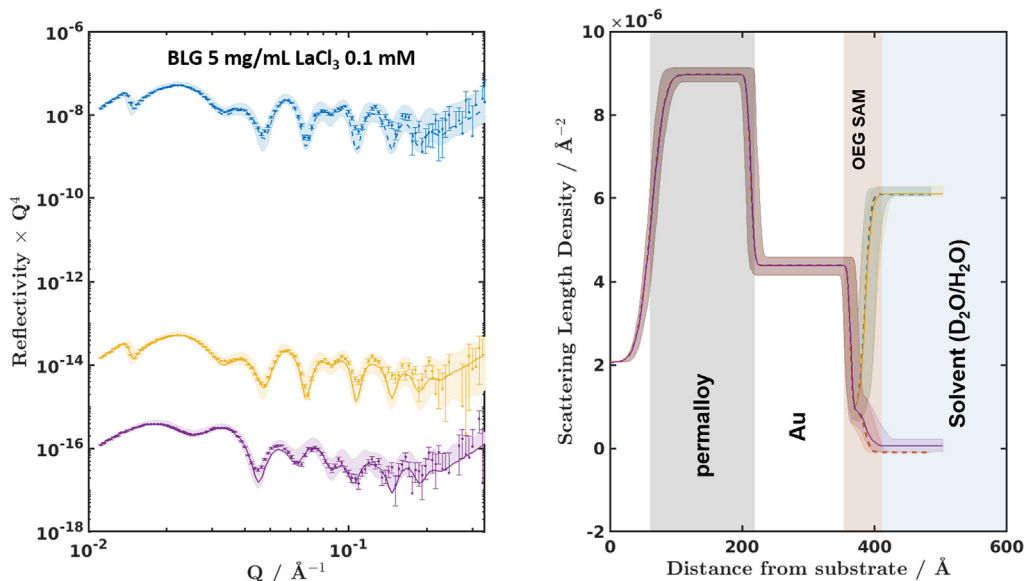


Fig. 3. Regime I: Neutron reflectivity data and fits (left) and corresponding scattering length density profiles (right) for a SAM exposed to 5 mg/mL BLG at 0.1 mM LaCl₃ (in D₂O(l) (yellow curve) and in H₂O(l) (purple curve)). The shaded regions indicate the 95% CI given by a Bayesian error analysis. The plots include the bare SAM in D₂O(l) (blue curve), i.e. prior to the addition of BLG solution. In this series the no protein data set in H₂O(l) is missing due to loss of beamtime. The model used, included an additional layer representing potential BLG adsorption - the layer hydration was close to 100% indicating the absence of adsorption.

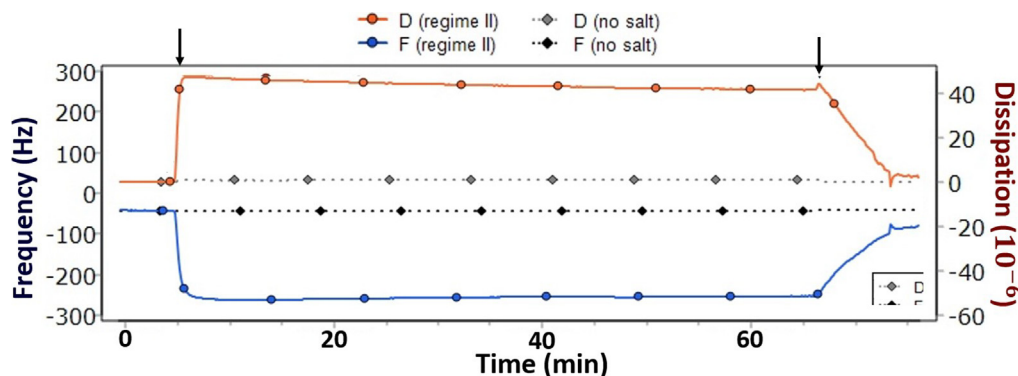


Fig. 4. Regime II: QCM-D raw data on a thiol-coated gold surface with the frequency shifts (blue) and the dissipation shifts (red) of the 9th overtone showing the system with 5 mg/mL of BLG in D₂O(l) at 0.8 mM LaCl₃ concentration. For comparison, a measurement without salt and 5 mg/ml BLG (i.e. protein resistance) is plotted in the figure showing a frequency shift (dotted black) and dissipation (dotted gray). In the first 5 min, the system is equilibrated in D₂O(l) and rinsed again with D₂O(l) after ~65 min (see arrows). A large decrease in frequency is visible, as well as a large increase in dissipation, suggesting a thick, hydrated protein layer.

aggregates from solution instead of individual proteins; this behaviour was observed on other surfaces as well [52].

The significant roughness extracted from the NR fit indicates a rather broad or diffuse protein/solution interface, as expected for adsorption in regime II (cf. Refs. [44,52]).

Concerning the dissipation, an increase up to a maximum of $\sim 50 \times 10^{-6}$ directly after the addition of the protein/salt solution is observed, which then slowly drops down to $\sim 40 \times 10^{-6}$. This trend of the dissipation curve indicates varying viscoelastic properties and in general a highly viscoelastic layer. After one hour of protein adsorption and by rinsing the QCM-D cell with water, the frequency and dissipation values are decreasing but not returning to the initial value (Fig. 4, from ~65 min to 80 min), indicating a significant amount of irreversibly bound proteins on the surface.

2.6. Regime III: Weak adsorption (attractive protein-protein interactions)

By further increasing the salt concentration up to 5 mM, regime III is reached, where – in the bulk – the solution becomes clear

again due to the charge reversal on the protein surface. The QCM-D raw data (Fig. 6) show lower Δf and ΔD in regime III (compared to regime II, 0.8 mM), but still larger compared to no salt and regime I (0.1 mM). This suggests at least some protein adsorption in the QCM-D in regime III. Modelling the QCM-D raw data revealed a ‘wet’ protein layer thickness of $d_{\text{QCM-D}}(5 \text{ mM}) = 28 \pm 16 \text{ \AA}$ for regime III, which is significantly thicker than in regime I ($d_{\text{QCM-D}}(0.1 \text{ mM})$), in which we observed no protein adsorption at all. Since the radius of BLG was calculated to be 23.5 \AA [53], the protein layer thickness $d_{\text{QCM-D}}$ in regime III seems to correspond to about one monolayer of proteins adsorbed on the surface. The protein layer thickness observed with NR in regime III is lower than the thickness measured with QCM-D. The protein layer morphology observed by NR in regime III is similar that in regime I, although a very slight thickness increase is observed: $d_{\text{NR}}(5.0 \text{ mM}) = 23 \text{ \AA}$, 95% CI [10,38] \AA compared to $d_{\text{NR}}(0.1 \text{ mM}) = 17 \text{ \AA}$, 95% CI [10,21] \AA . In both cases (regimes I and III) the layer is highly hydrated, indicating very little or no adsorption. The low protein layer roughness of 7 \AA , 95% CI [3,9] \AA confirms an ordered protein layer which is in line with protein monolayer adsorption and both the QCM-D data as well as the NR results indi-

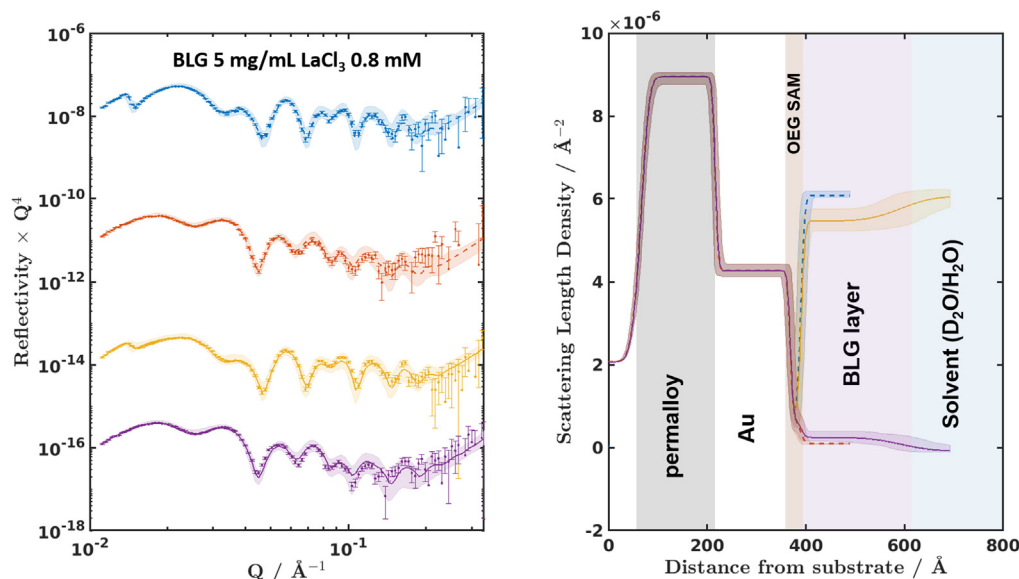


Fig. 5. Regime II: Neutron reflectivity data and fits (left) and corresponding scattering length density profiles (right) for a SAM exposed to 5 mg/mL BLG at 0.8 mM $LaCl_3$ (in $D_2O(l)$ (yellow curve) and in $H_2O(l)$ (purple curve)). The plots include the bare SAM in $D_2O(l)$ (blue curve) and $H_2O(l)$ (red curve), i.e. prior to the addition of BLG solution. The shaded regions indicate the 95% CI given by a Bayesian error analysis.

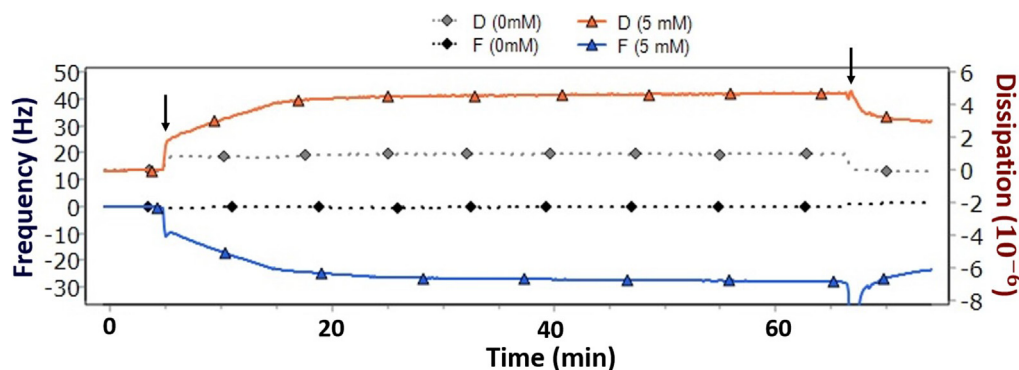


Fig. 6. Regime III: QCM-D raw data on a thiol-coated gold surface with the frequency shifts (blue) and the dissipation shifts (red) of the 9th overtone showing the system with 5 mg/mL of BLG in $D_2O(l)$ at 5.0 mM $LaCl_3$ concentration. For reference, a measurement without salt and 5 mg/mL BLG (i.e. protein resistance) is plotted in the figure showing a frequency shift (dotted black) and dissipation (dotted gray). In the first 5 min, the system is equilibrated in $D_2O(l)$ and rinsed again with $D_2O(l)$ after ~ 65 min (see arrows). A moderate decrease in frequency is visible, as well as a some increase in dissipation.

cate that the effect of re-entrant interface adsorption behavior found by Fries et al. [44] is also present in this system with a different surface. Hence, the decreased amount of adsorbed protein on the surface in regime III can be explained by charge inversion of the proteins (and the interface). The trivalent ions change the charge of the proteins from net negative to net positive by binding to the protein and also could potentially invert the surface charge of the OEG SAM. Due to the high ion concentration, binding sites on the proteins, as well as on the interface are already occupied with ions. This prevents multilayer formation and only allows a protein monolayer formation since the patches of the protein in the bulk and on the surface are already occupied by La^{3+} ions. This trend has already been observed for silicon dioxide surfaces [44] as well, suggesting a universal trend for negatively charged interfaces exposed to trivalent ions, as well as that this trend, dominated by electrostatic interactions, is guiding the bulk and interface behaviour of proteins (see Fig. 7).

2.7. Discussion

The parameters of the adsorbed protein layer as a function of added trivalent salt concentration are summarised in Table 1.

The thickness values from the QCM-D measurements are listed separately for $H_2O(l)$ and $D_2O(l)$, while the NR values were obtained by simultaneously fitting both solvent contrasts. The fact that the QCM-D values are very close to each other within error, demonstrates further that the layer morphology can be assumed to be very similar in both solvents. It is clear that the OEG SAM is protein resistant without added salt. The quality of the SAM structure and protein resistant properties were assessed for each sample individually through contact angle, AFM and PM-IRRAS measurements (see SI for more information), as well as a protein resistance QCM-D test (cf. Figure S5). In regime I, the QCM-D still gives a value consistent with no or very little adsorption, while the NR data fit reveals a 'layer' of $\sim 17 \text{\AA}$ thickness; this layer however has to be considered in the context of having $\sim 99\%$ hydration, which makes the values fully consistent with the QCM-D finding. It should be pointed out that we deliberately included a protein layer in the NR model for all salt concentrations in order to avoid bias and to be consistent across all salt concentrations. A fit without the additional layer does also fit the data (data not shown).

The same applies to the NR fit values for regime III. Here however (regime III), the QCM-D does show a layer which is not consistent with no adsorption, although the thickness is of the order of

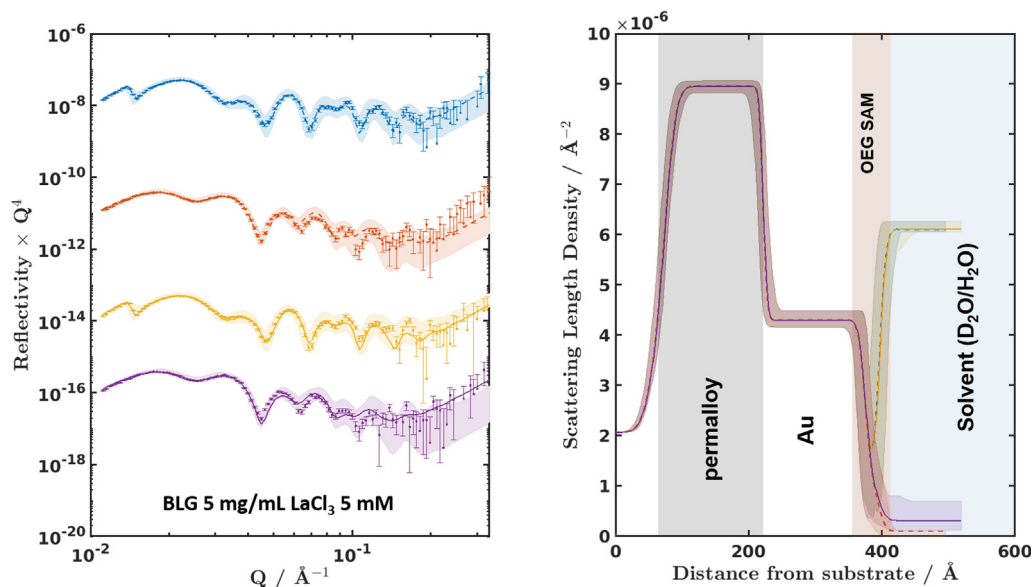


Fig. 7. Regime III: Neutron reflectivity data and fits (left) and corresponding scattering length density profiles (right) for a SAM exposed to 5 mg/mL BLG at 5.0 mM $LaCl_3$ (in $D_2O(l)$) (yellow curve) and in $H_2O(l)$ (purple curve)). The plots include the bare SAM in $D_2O(l)$ (blue curve) and $H_2O(l)$ (red curve), i.e. prior to the addition of BLG solution. The shaded regions indicate the 95% CI given by a Bayesian error analysis. The model used included a single layer representing potential BLG adsorption - the layer hydration was close to 100% indicating the absence of protein adsorption.

less than one protein diameter (23.5 \AA). This can have several reasons: QCM-D thickness values obtained from fitting to a Kelvin-Voigt model typically give a larger value than the thickness value obtained from NR due to hydration. In addition, both the QCM-D and NR values have relatively large error bars. This suggests that both techniques are at their sensitivity limit (i.e. measuring less than $\sim 10\%$ coverage of protein). QCM-D sensors are also known to have a larger roughness than typical NR samples (cf. Figure S3). The larger roughness means larger specific surface area and can thus lead to enhanced adsorption compared to a smoother surface. The area sampled by NR was also much larger (18 cm^2 compared to $\sim 0.25 cm^2$ for QCM-D). Furthermore, the QCM-D frequency shift in regime III was reduced to about half after rinsing with pure solvent. This suggests that a large proportion of proteins are only loosely bound and/or may be highly hydrated. NR may not be sufficiently sensitive to detect such a highly hydrated layer. This could explain the difference in values between the two techniques in regime III. It should be noted however, that the NR raw data in regimes I and III do not display differences outside the error bars when compared to each other and also to the SAM without protein exposure.

Importantly, the situation is substantially different in regime II. In this regime, where the SAM's protein resistance clearly breaks down, both techniques show a thick (multiple protein diameters) and hydrated adsorption layer. As mentioned before, in this case the difference in thickness can be explained by the fact that the QCM-D value includes the mass of bound hydration water, while the NR yields the 'dry' thickness with the hydration (and roughness) as separate parameters.

Since protein resistance is still present in regime I, a critical concentration of trivalent salt seems to be needed to overcome the protein-repellent properties. A replacement of the structured water molecules, coupled in an interfacial water layer to the SAM (cf. Refs. [9,10,12]) by trivalent ions is therefore proposed to be a possible mechanism in overcoming the protein resistance. Through the addition of a sufficient amount of salt, the water molecules coupled to the layer are increasingly replaced by ions and protein-ion complexes electrostatically bound to the SAM surface. This would lead to a replacement of the interfacial water layer. This

water replacement as well as further ions forming positively charged anchor points for proteins to bind would have two effects. On the one hand, the weakening of the repulsive forces by displacing water molecules from the structured and tightly bound water layer. On the other hand, the creation of an attractive, electrostatic force between the SAM, positively charged La^{3+} ions and the negatively charged proteins in bulk. The massive increase in regime II could then be explained by protein multilayer formation, in which ions not only mediate protein-surface bridging but also protein-protein bridging as it is the case on a bare SiO_2 surface [44]. In the end, this leads to a continuously increasing mass and a constantly increasing layer thickness [39].

3. Summary and conclusion

By using a combination of QCM-D and NR, we show for the first time the breakdown of protein resistance in normally protein resistant OEG based SAMs through the use of trivalent salt. The SAMs retained their non-fouling properties under no salt or a low salt solvent conditions in the presence of a 5 mg/mL BLG solution. This is consistent with previous reports using EG_3OH SAMs in combination with different types of proteins [9,10]. By increasing the amount of salt to 0.8 mM (regime II), protein resistance broke down and a large amount of protein adsorbed to the surface. This indicated that a critical amount of trivalent salt is needed to overcome the non-fouling properties. Water molecules tightly bound and located in the interfacial water region are assumed to be one key factor for achieving protein resistance. Hence, alterations of these non-fouling properties are suspected to be facilitated by protein-ion complexes replacing these water molecules coupled to the SAM. Simultaneously, the ions serve as ion bridges between the net negatively charged proteins and the SAM layer resulting in a protein multilayer formation in regime II. In regime III ($c_s = 5.0 mM$), the adsorbed amount was decreasing substantially compared to the maximum in regime II. Such behavior indicates the presence of re-entrant interface adsorption in this system (presumably due to charge inversion on the protein surface). Concerning the properties of the protein layer, a relatively high dissipation shift in regime II indicated a very soft and viscoelastic protein layer

with plenty of water molecules still incorporated in the protein layer between the SAM molecules and coupled to the protein layer. This is confirmed by the NR data, which show a relatively high hydration of the protein layer.

To our knowledge, this is the first observation of the breakdown of protein resistance of a normally protein resistant OEG SAM induced by the addition of a trivalent salt. This finding adds to the still incomplete picture of the mechanism by which short chained, OEG terminated SAMs are able to resist the non-specific adsorption of proteins. It is known from other studies [54] on related bulk systems, that protein-trivalent ion mixtures exhibit many interesting features, including re-entrant condensation, liquid-liquid phase separation, pronounced temperature dependence etc. Future work will explore the details of the interactions in this complex system by investigating the universality (different proteins and trivalent salts) of the phenomenon and by studying the impact of other parameters, such as temperature and pH, and also by using different protein resistant SAMs. In this context, it will be interesting to determine, if a wetting transition can be observed under certain conditions, as is the case for a bare silica interface [39]. Due to the ability of BLG to crystallise in regime II, this interface may be of interest in the context of bulk/surface nucleation as a pathway to crystallisation.

4. Experimental

4.1. Materials

BLG (90%, product No. L3908) powder purchased from Merck KGaK was dissolved in degassed H₂O(l) (Milli-Q water, Millipore, 18.2 MΩ cm) or D₂O(l) (Merck KGaK, Atom% D ≥ 99.9%, product No. 151882) for the stock solution preparation. The protein concentration c_p of these stock solutions was determined with the UV-vis spectrometer (Cary 50 UV-vis spectrometer, Varian Inc., now Agilent Technologies), via the Beer-Lambert law and the protein-specific extinction coefficient for BLG of 0.96 mL/(mg*cm) [55]. Three different dilutions were measured to determine the final, averaged concentration of the stock solution. Each stock solution was stored at 8 °C and used within two weeks to avoid contamination with bacteria. LaCl₃ used in this study was purchased from Merck KGaK with a stated purity of ≥ 99.99% (product No. 449830). The salt stock solution used for the experiments was prepared at a concentration c_s of 100 mM by dissolving the anhydrous beads in degassed H₂O(l) (Milli-Q water, Millipore, 18.2 MΩ cm) or D₂O(l) (Merck KGaK, ATOM% D ≥ 99.9%). Triethylene glycol mono-11-mercaptoundecyl ether (SH(CH₂)₁₁EG₃OH) purchased from Pro-Chimia Surfaces with a purity of >95% and a density of $\rho = 1.03$ g/cm³ (product no: TH 001-m11.n3) was used in this study. The pure alkanethiols were stored under argon atmosphere at -18 °C. For the substrate coating with SAMs, an alkanethiol concentration of 500 μM in a degassed ethanol (Merck KGaK, purity ≥ 99.5%) solution was prepared.

4.2. Substrate preparation

For the NR measurements, ozone cleaned silicon crystals (50 × 80 × 15 mm) with a polished 80 × 50 mm face (111 orientation, surface roughness (RMS) ~3 Å) were sputter-coated with permalloy (Ni80Fe20) and gold (approximately 15 nm thickness each) at the NIST center for Nanoscience and Technology, Gaithersburg, MD, U.S.A., in a Denton Discovery 550 sputtering chamber. For the QCM-D measurements, gold coated quartz-crystal sensors used were ordered from QSense (QSX-301 Gold) with a surface roughness, specified by QSense, of less than 1 nm. All substrates were exposed to UV/ozone for 15 min, immediately rinsed with

Milli-Q water and dried in a gentle nitrogen stream. Substrates were then submerged in the OEG thiol solution directly after cleaning and were incubated under argon atmosphere at room temperature and in the dark for 18 h. After this defined immersion time, substrates were removed from solution, rinsed with ethanol and dried with nitrogen. The coated substrates were stored under argon in the dark at 8 °C until the measurements were performed (for a maximum of two days).

4.3. Quartz-crystal microbalance with dissipation (QCM-D)

Measurements were executed at 20 °C with the QSense Explorer from Biolin Scientific. The device has one QCM-D chamber with a total volume of about 200 μL, the volume above the sensor is about 40 μL. The theoretical sensitivity of the device operating in liquid is specified by Biolin Scientific with about 1.8 ng/cm². For all measurements the QCM-D flow cell was used in upside-down configuration to avoid sedimentation during the adsorption process. Depending on the solvent used in the measurement, H₂O(l) or D₂O(l) was pumped into the cell at the beginning of each measurement to calibrate the system. After the signal had stabilized, around 4 mL of protein solution was pumped into the QCM-D cell. The adsorption process was observed for one hour, followed by a rinsing step with the pure solvent. Data analysis was executed with the QSense analysis software QTools and Dfind. Viscoelastic modeling (Kelvin-Voigt model) was employed, since the Sauerbrey equation is not valid for the measured samples ($D \neq 0$) [56,57]. The layer density was set to 1200 kg/m³, fluid density either to 1106 kg/m³ for D₂O(l) or to 998 kg/m³ for H₂O(l) [58,35]. The range of the layer viscosity was set to 0.0001–0.01 kg/ms, layer shear modulus to 10⁴–10⁸ Pa and layer thickness to 10⁻¹¹–10⁻⁶ m. Prior to each measurement, the quality of the SAM layer was determined by contact angle, AFM and PM-IRRAS measurements, as well as a protein resistance QCM test (more information can be found in the SI, Figure S5). The QCM-D adsorption measurements were tested for reproducibility, by repeating measurements at least three times. The errors given are the standard deviations of these measurements. For certain conditions, where there was no or very little BLG adsorption, fitting via the Kelvin-Voigt model did not yield meaningful results.

4.4. Neutron reflectivity (NR)

Specular neutron reflectometry (NR) measurements were carried out using the PolRef time-of-flight reflectometer at the ISIS spallation source, Rutherford Appleton Laboratory (Oxfordshire, UK) [59]. A broad band neutron beam with wavelengths from 1 to 12 Å was used. The reflected intensity is measured as a function of the momentum transfer $Q_z = \frac{4\pi}{\lambda} \sin(\theta)$, where λ is wavelength and θ is the incident angle. The collimated neutron beam was reflected from the silicon-liquid interface at different glancing angles of $\theta = 0.6$ and 2.3° in order to cover the desired Q range, i.e. from total reflection edge to background. The solvent exchange set-up is described in previous publications [40,60,61]. Purpose-built liquid flow cells for analysis of the silicon-liquid interface were placed on a variable angle sample stage in the NR instrument and the inlet to the liquid cell was connected to a liquid chromatography pump (JASCO PU-4180), which allowed the automated exchange of the solution isotopic contrast within the (3 mL volume) solid-liquid sample cell. For each solution isotopic contrast change, a total of 10 mL solution (BLG/salt/H₂O(l) or BLG/salt/D₂O(l)) was pumped through the cell at a speed of 1.5 mL/min. First, the salt/protein mixture in D₂O(l) was pumped into the cell and after 20 min of equilibration the first neutron reflectivity mea-

surement was started. We made use of the solvent contrast effect by exchanging from D₂O(l) to H₂O(l).

4.5. Neutron reflectivity data analysis

Data analysis on similar systems is described in previous publications [60,61]. In brief, neutron reflectivity data were analyzed using the RasCAL2019 software package [62], in which models representing the interfacial out-of-plane structure are fitted to the data using an optical matrix formalism [63]. The interface is described as a series of slabs, each of which is characterized by its scattering length density (SLD), thickness, and roughness. Interfacial roughness represented as an error function, according to the approach by Nevot and Croce [64], but re-sampled in RasCAL in terms of thin slabs with zero roughness, thus allowing roughnesses, which are of the order of the layer thickness. The reflectivity for an initial model based on known sample parameters, such as substrate, its oxide layer, permalloy, gold and SAM layer as well as the solvent is calculated and compared with the experimental data. A protein layer was modelled as a single slab of either the SLD which BLG assumes in D₂O(l) or that in H₂O(l), a layer roughness and a hydration parameter. Four data sets (SAM only in D₂O(l) and H₂O(l), SAM exposed to respective protein solution in D₂O(l) and H₂O(l)) were co-refined, unless otherwise stated. All fitted model parameters are shown in the supporting information. A least-squares minimization is used to adjust the fit parameters to reduce the differences between the model reflectivity and the data. In all cases the simplest possible model (i.e. least number of layers), which adequately described the data, was selected. Error analysis of the fitted parameters was carried out using Rascal's "Bayesian" error algorithm using a Monte Carlo Markov Chain (MCMC). For the sampling, 20000 MCMC points were used as well as 1500 "burn in" points and the run was repeated 12 times. The resulting plots contain fits and corresponding real space structure of the sample layer system, as well as 95% confidence intervals (shown as shaded regions).

CRediT authorship contribution statement

Maximilian W. A. Skoda: Conceptualization, Methodology, Validation, Software, Formal analysis, Investigation, Funding acquisition, Resources, Data Curation, Writing – original draft, Visualisation; **Nina F. Conzelmann:** Formal analysis, Investigation, Writing, Visualisation, Writing – original draft. **Madeleine R. Fries:** Conceptualization, Methodology, Validation, Formal analysis, Investigation, Writing – review & editing, Visualisation. **Lara F. Reichart:** Formal analysis, Investigation, Writing – review & editing. **Robert M. J. Jacobs:** Conceptualization, Methodology, Formal analysis, Investigation, Data Curation, Writing – review & editing. **Fajun Zhang:** Validation, Resources, Supervision, Writing – review & editing. **Frank Schreiber:** Conceptualization, Project administration, Funding acquisition, Resources, Data Curation, Writing – review & editing, Supervision.

Declaration of Competing Interest

The authors declare that they have no known competing financial interests or personal relationships that could have appeared to influence the work reported in this paper.

Acknowledgement

The authors acknowledge financial support by the DFG. C. Kinane and A. Caruana (ISIS Neutron and Muon Source) are gratefully acknowledged for beam time support. We thank ISIS/STFC

(Experiment number RB1910571; <https://doi.org/10.5286/ISIS.E.RB1910571-1>) for access to neutron beam time. M.W.A.S. is indebted to A. Church and the soft-matter team for the provision of solid-liquid interface cells. We also thank L. Clifton for constructive discussions and help with NR substrates and SAM fabrication. We thank Professor Frank Heinrich and the NIST Nano-fabrication facility (project number N16.0028.05) for the metal coatings used in the NR samples described in this study.

Appendix A. Supplementary material

Supplementary data associated with this article can be found, in the online version, at <https://doi.org/10.1016/j.jcis.2021.08.018>.

References

- [1] K.M. Hansson, S. Tosatti, J. Isaksson, J. Wetterö, M. Textor, T.L. Lindahl, P. Tengvall, Whole blood coagulation on protein adsorption-resistant peg and peptide functionalised peg-coated titanium surfaces, *Biomaterials* 26 (8) (2005) 861–872, <https://doi.org/10.1016/j.biomaterials.2004.03.036>. URL <https://www.sciencedirect.com/science/article/pii/S0142961204002947>.
- [2] M. Rabe, D. Verdes, S. Seeger, Understanding protein adsorption phenomena at solid surfaces, *Adv. Colloid Interface Sci.* 162 (1) (2011) 87–106, <https://doi.org/10.1016/j.cis.2010.12.007>. URL <http://www.sciencedirect.com/science/article/pii/S0001868611000066>.
- [3] A. Hausmann, P. Sanciolo, T. Vasiljevic, M. Weeks, K. Schroën, S. Gray, M. Duke, Fouling of dairy components on hydrophobic polytetrafluoroethylene (ptfe) membranes for membrane distillation, *J. Membr. Sci.* 442 (2013) 149–159, <https://doi.org/10.1016/j.memsci.2013.03.057>. URL <http://www.sciencedirect.com/science/article/pii/S0376738813002603>.
- [4] A.W. Mohammad, C.Y. Ng, Y.P. Lim, G.H. Ng, Ultrafiltration in food processing industry: review on application, membrane fouling, and fouling control, *Food Bioproc. Tech.* 5 (4) (2012) 1143–1156.
- [5] B.J. James, Y. Jing, X. Dong Chen, Membrane fouling during filtration of milk—a microstructural study, *J. Food Eng.* 60 (4) (2003) 431–437, [https://doi.org/10.1016/S0260-8774\(03\)00066-9](https://doi.org/10.1016/S0260-8774(03)00066-9). URL <http://www.sciencedirect.com/science/article/pii/S0260877403000669>.
- [6] B. Zhou, J.T. Tobin, S. Drusch, S.A. Hogan, Interfacial properties of milk proteins: A review, *Adv. Colloid Interface Sci.* (2020) 102347, <https://doi.org/10.1016/j.cis.2020.102347>. URL <https://www.sciencedirect.com/science/article/pii/S0001868620306163>.
- [7] D. Rana, T. Matsuura, Surface modifications for antifouling membranes, *Chem. Rev.* 110 (4) (2010) 2448–2471, <https://doi.org/10.1021/cr800208y>. URL <https://doi.org/10.1021/cr800208y>.
- [8] R.L.C. Wang, H.J. Kreuzer, M. Grunze, Molecular conformation and solvation of oligo(ethylene glycol)-terminated self-assembled monolayers and their resistance to protein adsorption, *J. Phys. Chem. B* 101 (47) (1997) 9767–9773, <https://doi.org/10.1021/jp9716952>. URL <https://doi.org/10.1021/jp9716952>.
- [9] T. Hayashi, Y. Tanaka, Y. Koide, M. Tanaka, M. Hara, Mechanism underlying bioinertness of self-assembled monolayers of oligo(ethyleneglycol)-terminated alkanethiols on gold: protein adsorption, platelet adhesion, and surface forces, *Phys. Chem. Chem. Phys.* 14 (2012) 10196–10206, <https://doi.org/10.1039/C2CP41236E>. URL <https://doi.org/10.1039/C2CP41236E>.
- [10] S. Herrwerth, W. Eck, S. Reinhardt, M. Grunze, Factors that determine the protein resistance of oligoether self-assembled monolayers – internal hydrophilicity, terminal hydrophilicity, and lateral packing density, *J. Am. Chem. Soc.* 125 (31) (2003) 9359–9366, <https://doi.org/10.1021/ja034820y>. URL <https://doi.org/10.1021/ja034820y>.
- [11] K. Prime, G. Whitesides, Self-assembled organic monolayers: model systems for studying adsorption of proteins at surfaces, *Science* 252 (5009) (1991) 1164–1167, <https://doi.org/10.1126/science.252.5009.1164>. arXiv: <https://science.sciencemag.org/content/252/5009/1164.full.pdf>, <https://science.sciencemag.org/content/252/5009/1164>.
- [12] P. Harder, M. Grunze, R. Dahint, G.M. Whitesides, P.E. Laibinis, Molecular conformation in oligo(ethylene glycol)-terminated self-assembled monolayers on gold and silver surfaces determines their ability to resist protein adsorption, *J. Phys. Chem. B* 102 (2) (1998) 426–436, <https://doi.org/10.1021/jp972635z>. URL <https://doi.org/10.1021/jp972635z>.
- [13] K.L. Prime, G.M. Whitesides, Adsorption of proteins onto surfaces containing end-attached oligo(ethylene oxide): a model system using self-assembled monolayers, *J. Am. Chem. Soc.* 115 (23) (1993) 10714–10721, <https://doi.org/10.1021/ja00076a032>. URL <https://doi.org/10.1021/ja00076a032>.
- [14] K. Feldman, G. Hähner, N.D. Spencer, P. Harder, M. Grunze, Probing resistance to protein adsorption of oligo(ethylene glycol)-terminated self-assembled monolayers by scanning force microscopy, *J. Am. Chem. Soc.* 121 (43) (1999) 10134–10141, <https://doi.org/10.1021/ja991049b>. URL <https://doi.org/10.1021/ja991049b>.
- [15] P. Zhang, B.D. Ratner, A.S. Hoffman, S. Jiang, 1.4.3a – nonfouling surfaces, in: W. R. Wagner, S.E. Sakiyama-Elbert, G. Zhang, M.J. Yaszemski (Eds.), *Biomaterials Science*, fourth ed., Academic Press, 2020, pp. 507–513. doi: 10.1016/B978-0-

- 12-816137-1.00034-9. URL <https://www.sciencedirect.com/science/article/pii/B9780128161371000349>.
- [16] X. Han, Z. Yuan, Y. Niu, X. Chen, H. Liu, Surface modification by poly(ethylene glycol) with different end-grafted groups: Experimental and theoretical study, *Biointerphases* 16 (2) (2021) 021002, <https://doi.org/10.1116/6.0000647>.
- [17] S. Jeon, J. Lee, J. Andrade, P. De Gennes, Protein–surface interactions in the presence of polyethylene oxide: I. Simplified theory, *J. Colloid Interface Sci.* 142 (1) (1991) 149–158, <https://doi.org/10.1016/0021-9797>. <http://www.sciencedirect.com/science/article/pii/0021979791900438>.
- [18] L. Li, S. Chen, J. Zheng, B.D. Ratner, S. Jiang, Protein adsorption on oligo(ethylene glycol)-terminated alkanethiolate self-assembled monolayers: The molecular basis for nonfouling behavior, *J. Phys. Chem. B* 109 (7) (2005) 2934–2941, <https://doi.org/10.1021/jp0473321>. URL <https://doi.org/10.1021/jp0473321>.
- [19] M.W.A. Skoda, R.M.J. Jacobs, J. Willis, F. Schreiber, Hydration of oligo(ethylene glycol) self-assembled monolayers studied using polarization modulation infrared spectroscopy, *Langmuir* 23 (3) (2007) 970–974, <https://doi.org/10.1021/la0616653>. URL <https://doi.org/10.1021/la0616653>.
- [20] J.M. Harris, S. Zalipsky, Poly(ethylene glycol): Chemistry and biological applications, *ACS Symp. Ser.* (1997).
- [21] A. Rosenhahn, S. Schilp, H.J. Kreuzer, M. Grunze, The role of “inert” surface chemistry in marine biofouling prevention, *Phys. Chem. Phys.* 12 (2010) 4275–4286, <https://doi.org/10.1039/C001968M>. URL <https://doi.org/10.1039/C001968M>.
- [22] R.Y. Wang, M. Himmelhaus, J. Fick, S. Herrwerth, W. Eck, M. Grunze, Interaction of self-assembled monolayers of oligo(ethylene glycol)-terminated alkanethiols with water studied by vibrational sum-frequency generation, *J. Chem. Phys.* 122 (16) (2005) 164702, <https://doi.org/10.1063/1.1869414>.
- [23] M. Zolk, F. Eisert, J. Pipper, S. Herrwerth, W. Eck, M. Buck, M. Grunze, Solvation of oligo(ethylene glycol)-terminated self-assembled monolayers studied by vibrational sum frequency spectroscopy, *Langmuir* 16 (14) (2000) 5849–5852, <https://doi.org/10.1021/la0003239>. URL <https://doi.org/10.1021/la0003239>.
- [24] C. Dicke, G. Hähner, pH-dependent force spectroscopy of tri(ethylene glycol)- and methyl-terminated self-assembled monolayers adsorbed on gold, *J. Am. Chem. Soc.* 124 (42) (2002) 12619–12625, <https://doi.org/10.1021/ja027447n>. URL <https://doi.org/10.1021/ja027447n>.
- [25] H.J. Kreuzer, R.L.C. Wang, M. Grunze, Hydroxide ion adsorption on self-assembled monolayers, *J. Am. Chem. Soc.* 125 (27) (2003) 8384–8389, <https://doi.org/10.1021/ja0350839>. URL <https://doi.org/10.1021/ja0350839>.
- [26] C. Dicke, G. Hähner, Interaction between a hydrophobic probe and tri(ethylene glycol)-containing self-assembled monolayers on gold studied with force spectroscopy in aqueous electrolyte solution, *J. Phys. Chem. B* 106 (17) (2002) 4450–4456, <https://doi.org/10.1021/jp013809m>. URL <https://doi.org/10.1021/jp013809m>.
- [27] M.W.A. Skoda, F. Schreiber, R.M.J. Jacobs, J.R.P. Webster, M. Wolff, R. Dahint, D. Schwendel, M. Grunze, Protein density profile at the interface of water with oligo(ethylene glycol) self-assembled monolayers, *Langmuir* 25 (7) (2009) 4056–4064, <https://doi.org/10.1021/la8028534>. URL <https://doi.org/10.1021/la8028534>.
- [28] J. Zheng, L. Li, H.-K. Tsao, Y.-J. Sheng, S. Chen, S. Jiang, Strong repulsive forces between protein and oligo(ethylene glycol) self-assembled monolayers: A molecular simulation study, *Biophys. J.* 89 (1) (2005) 158–166, <https://doi.org/10.1529/biophysj.105.059428>. <http://www.sciencedirect.com/science/article/pii/S0006349505726679>.
- [29] M. Tanaka, S. Morita, T. Hayashi, Role of interfacial water in determining the interactions of proteins and cells with hydrated materials, *Colloids Surf. B: Biointerfaces* 198 (2021) 111449, <https://doi.org/10.1016/j.colsurfb.2020.111449>. <http://www.sciencedirect.com/science/article/pii/S0927776520308055>.
- [30] Y. Xie, W. Gong, J. Jin, Z. Zhao, Z. Li, J. Zhou, Molecular simulations of lysozyme adsorption on an electrically responsive mixed self-assembled monolayer, *Appl. Surf. Sci.* 506 (2020) 144962, <https://doi.org/10.1016/j.apsusc.2019.144962>. <http://www.sciencedirect.com/science/article/pii/S0169433219337791>.
- [31] A. Vaish, D.J. Vanderah, R. Vierling, F. Crawshaw, D.T. Gallagher, M.L. Walker, Membrane protein resistance of oligo(ethylene oxide) self-assembled monolayers, *Colloids Surf. B: Biointerfaces* 122 (2014) 552–558, <https://doi.org/10.1016/j.colsurfb.2014.07.031>. <http://www.sciencedirect.com/science/article/pii/S0927776514004020>.
- [32] L. Li, S. Chen, S. Jiang, Protein interactions with oligo(ethylene glycol) (oeg) self-assembled monolayers: Oeg stability, surface packing density and protein adsorption, *J. Biomater. Sci. Polym. Ed.* 18 (11) (2007) 1415–1427, <https://doi.org/10.1163/156856207782246795>. pMID: 17961324.
- [33] R. Schlapak, D. Armitage, N. Saucedo-Zeni, W. Chrzanowski, M. Hohage, D. Caruana, S. Howorka, Selective protein and dna adsorption on pll-peg films modulated by ionic strength, *Soft Matter* 5 (2009) 613–621, <https://doi.org/10.1039/B815065F>. URL <https://doi.org/10.1039/B815065F>.
- [34] F.A.M. Leermakers, M. Ballauff, O.V. Borisov, On the mechanism of uptake of globular proteins by polyelectrolyte brushes: a two-gradient self-consistent field analysis, *Langmuir* 23 (7) (2007) 3937–3946, <https://doi.org/10.1021/la0632777>. URL <https://doi.org/10.1021/la0632777>.
- [35] J. Kim, N. Weber, G. Shin, Q. Huang, S. Liu, The study of β -lactoglobulin adsorption on polyethersulfone thin film surface using qcm-d and afm, *J. Food Sci.* 72 (4) (2007) E214–E221, <https://doi.org/10.1111/j.1750-3841.2007.00344.x>. <https://onlinelibrary.wiley.com/doi/abs/10.1111/j.1750-3841.2007.00344.x>.
- [36] Özgür Coskun, Ibrahim Gülseren, 5 - nanofibrils of beta-lactoglobulin for encapsulation of food ingredients, in: S.M. Jafari (Ed.), *Biopolymer Nanostructures for Food Encapsulation Purposes, Nanoencapsulation in the Food Industry*, Academic Press, 2019, pp. 125–146. doi:10.1016/B978-0-12-815663-6.00005-7. <https://www.sciencedirect.com/science/article/pii/B9780128156636000057>.
- [37] K. Broersen, Milk processing affects structure, bioavailability and immunogenicity of β -lactoglobulin, *Foods* 9 (7) (2020), <https://doi.org/10.3390/foods9070874>. <https://www.mdpi.com/2304-8158/9/7/874>.
- [38] A. Barbiroli, T. Beringhelli, F. Bonomi, D. Donghi, P. Ferranti, M. Galliano, S. lametti, D. Maggioni, P. Rasmussen, S. Scanu, M.C. Vilaro, Bovine beta-lactoglobulin acts as an acid-resistant drug carrier by exploiting its diverse binding regions, *Biol. Chem.* 391 (2010) 21–32.
- [39] M.R. Fries, D. Stopper, M.W.A. Skoda, M. Blum, C. Kertzschner, A. Hinderhofer, F. Zhang, R.M.J. Jacobs, R. Roth, F. Schreiber, Enhanced protein adsorption upon bulk phase separation, *Sci. Rep.* 10 (1) (2020) 10349, <https://doi.org/10.1038/s41598-020-66562-0>. URL <https://doi.org/10.1038/s41598-020-66562-0>.
- [40] M.R. Fries, M.W. Skoda, N.F. Conzelmann, R.M. Jacobs, R. Maier, N. Scheffczyk, F. Zhang, F. Schreiber, Bulk phase behaviour vs interface adsorption: Effects of anions and isotopes on β -lactoglobulin (blg) interactions, *J. Colloid Interface Sci.* (2021), <https://doi.org/10.1016/j.jcis.2021.04.011>. <https://www.sciencedirect.com/science/article/pii/S0021979721005002>.
- [41] O. Matsarskaia, F. Roosen-Runge, F. Schreiber, Multivalent ions and biomolecules: Attempting a comprehensive perspective, *ChemPhysChem* 21 (16) (2020) 1742–1767. arXiv: <https://chemistry-europe.onlinelibrary.wiley.com/doi/pdf/10.1002/cphc.202000162>. doi:10.1002/cphc.202000162. <https://chemistry-europe.onlinelibrary.wiley.com/doi/abs/10.1002/cphc.202000162>.
- [42] F. Roosen-Runge, B.S. Heck, F. Zhang, O. Kohlbacher, F. Schreiber, Interplay of ph and binding of multivalent metal ions: charge inversion and reentrant condensation in protein solutions, *J. Phys. Chem. B* 117 (18) (2013) 5777–5787.
- [43] F. Zhang, R. Roth, M. Wolf, F. Roosen-Runge, M.W.A. Skoda, R.M.J. Jacobs, M. Stzucki, F. Schreiber, Charge-controlled metastable liquid-liquid phase separation in protein solutions as a universal pathway towards crystallization, *Soft Matter* 8 (2012) 1313–1316, <https://doi.org/10.1039/C2SM07008A>. URL <https://doi.org/10.1039/C2SM07008A>.
- [44] M.R. Fries, D. Stopper, M.K. Braun, A. Hinderhofer, F. Zhang, R.M. Jacobs, M.W. Skoda, H. Hansen-Goos, R. Roth, F. Schreiber, Multivalent-ion-activated protein adsorption reflecting bulk reentrant behavior, *Phys. Rev. Lett.* 119 (22) (2017) 228001.
- [45] F. Zhang, M.W.A. Skoda, R.M.J. Jacobs, S. Zorn, R.A. Martin, C.M. Martin, G.F. Clark, S. Weggler, A. Hildebrandt, O. Kohlbacher, F. Schreiber, Reentrant condensation of proteins in solution induced by multivalent counterions, *Phys. Rev. Lett.* 101 (14) (2008), <https://doi.org/10.1103/PhysRevLett.101.148101>.
- [46] N. Bonnet, D. O'Hagan, G. Hähner, Protein adsorption onto cf3-terminated oligo(ethylene glycol) containing self-assembled monolayers (sams): the influence of ionic strength and electrostatic forces, *Phys. Chem. Chem. Phys.* 12 (2010) 4367–4374, <https://doi.org/10.1039/B923065N>. URL <https://doi.org/10.1039/B923065N>.
- [47] J. Yu, N.E. Jackson, X. Xu, Y. Morgenstern, Y. Kaufman, M. Ruths, J.J. de Pablo, M. Tirrell, Multivalent counterions diminish the lubricity of polyelectrolyte brushes, *Science* 360 (6396) (2018) 1434–1438. arXiv: <https://science.sciencemag.org/content/360/6396/1434.full.pdf>. doi:10.1126/science.aar5877. <https://science.sciencemag.org/content/360/6396/1434>.
- [48] J. Yu, J. Mao, G. Yuan, S. Satija, Z. Jiang, W. Chen, M. Tirrell, Structure of polyelectrolyte brushes in the presence of multivalent counterions, *Macromolecules* 49 (15) (2016) 5609–5617, <https://doi.org/10.1021/acs.macromol.6b01064>. URL <https://doi.org/10.1021/acs.macromol.6b01064>.
- [49] L. Korson, W. Drost-Hansen, F.J. Millero, Viscosity of water at various temperatures, *J. Phys. Chem.* 73 (1) (1969) 34–39, <https://doi.org/10.1021/j100721a006>.
- [50] G. Vinothkumar, S. Rengaraj, P. Arunkumar, S.W. Cha, K. Suresh Babu, Ionic radii and concentration dependency of re³⁺ (eu³⁺, nd³⁺, pr³⁺, and la³⁺)-doped cerium oxide nanoparticles for enhanced multizyme-mimetic and hydroxyl radical scavenging activity, *J. Phys. Chem. C* 123 (1) (2019) 541–553. doi:10.1021/acs.jpcc.8b10108. doi: 10.1021/acs.jpcc.8b10108.
- [51] K. Kandori, S. Toshima, M. Wakamura, M. Fukusumi, Y. Morisada, Effects of modification of calcium hydroxyapatites by trivalent metal ions on the protein adsorption behavior, *J. Phys. Chem. B* 114 (7) (2010) 2399–2404, <https://doi.org/10.1021/jp911783r>. URL <https://doi.org/10.1021/jp911783r>.
- [52] M.R. Fries, N.F. Conzelmann, L. Günter, O. Matsarskaia, M.W.A. Skoda, R.M.J. Jacobs, F. Zhang, F. Schreiber, Bulk phase behavior vs interface adsorption: Specific multivalent cation and anion effects on bsa interactions, *Langmuir* 37 (1) (2021) 139–150, pMID: 33393312. arXiv: <https://doi.org/10.1021/acs.langmuir.0c02618>. doi:10.1021/acs.langmuir.0c02618. doi: 10.1021/acs.langmuir.0c02618.
- [53] E. Schuster, A.-M. Hermansson, C. Ohgren, M. Rudemo, N. Lorén, Interactions and diffusion in fine-stranded β -lactoglobulin gels determined via frap and binding, *Biophys. J.* 106 (24411257) (2014) 253–262, <https://doi.org/10.1016/j.bpj.2013.11.2959>. <https://www.ncbi.nlm.nih.gov/pmc/articles/PMC3907260/>.
- [54] F. Zhang, F. Roosen-Runge, A. Sauter, M. Wolf, R.M. Jacobs, F. Schreiber, Reentrant condensation, liquid–liquid phase separation and crystallization in

- protein solutions induced by multivalent metal ions, *Pure Appl. Chem.* 86 (2) (2014) 191–202.
- [55] H.A. Sober, Handbook of biochemistry: selected data for molecular biology, Tech. rep., Chemical Rubber Co. (1968).
- [56] S.X. Liu, J.-T. Kim, Application of kevin–voigt model in quantifying whey protein adsorption on polyethersulfone using qcm-d, *J. Lab. Autom.* 14 (4) (2009) 213–220.
- [57] F. Höök, B. Kasemo, T. Nylander, C. Fant, K. Sott, H. Elwing, Variations in coupled water, viscoelastic properties, and film thickness of a mefp-1 protein film during adsorption and cross-linking: a quartz crystal microbalance with dissipation monitoring, ellipsometry, and surface plasmon resonance study, *Anal. Chem.* 73 (24) (2001) 5796–5804.
- [58] J.C. Crittenden, R.R. Trussell, D.W. Hand, K.J. Howe, G. Tchobanoglous, MWH's Water Treatment: Principles and Design, Third Edition: Principles and Design, Third Edition., John Wiley & Sons Inc, 2012.
- [59] T.R. Charlton, R.L.S. Coleman, R.M. Dalglish, C.J. Kinane, C. Neylon, S. Langridge, J. Plomp, N.G.J. Webb, J.R.P. Webster, Advances in neutron reflectometry at isis, *Neutron News* 22 (2) (2011) 15–18, <https://doi.org/10.1080/10448632.2011.569278>, arXiv:<https://doi.org/10.1080/10448632.2011.569278>, URL <https://doi.org/10.1080/10448632.2011.569278>.
- [60] L.A. Clifton, F. Ciesielski, M.W.A. Skoda, N. Paracini, S.A. Holt, J.H. Lakey, The effect of lipopolysaccharide core oligosaccharide size on the electrostatic binding of antimicrobial proteins to models of the gram negative bacterial outer membrane, *Langmuir* 32 (14) (2016) 3485–3494, <https://doi.org/10.1021/acs.langmuir.6b00240>.
- [61] L.A. Clifton, N. Paracini, A.V. Hughes, J.H. Lakey, N.-J. Steinke, J.F.K. Cooper, M. Gavutis, M.W.A. Skoda, Self-assembled fluid phase floating membranes with tunable water interlayers, *Langmuir* 35 (42) (2019) 13735–13744, <https://doi.org/10.1021/acs.langmuir.9b02350>.
- [62] A. Hughes., Rascal, Tech. rep. (2019). https://github.com/arwelHughes/RasCAL_2019.
- [63] M. Born, E. Wolf, Principles of Optics: Electromagnetic Theory of Propagation, Interference and Diffraction of Light, 6th Edition., Cambridge University Press, 1997.
- [64] Névot, L., Croce, P., Caractérisation des surfaces par réflexion rasante de rayons x. application à l'étude du polissage de quelques verres silicates, *Rev. Phys. Appl. (Paris)* 15(3) (1980) 761–779. doi:10.1051/rphysap:01980001503076100. doi: 10.1051/rphysap:01980001503076100.